Comparative dynamics analysis on xonotlite spherical particles synthesized via hydrothermal synthesis

F Liu[1, 2, 3], S Chen[1, 3], Q Lin[1, 2], X D Wang[2] and J X Cao[1, 2, 3, 4]

[1] School of Chemistry and Chemical Engineering, Guizhou University, Guiyang, Guizhou 550025, PR China
[2] Key Laboratory of Green Chemical and Clean Energy Technology, Guiyang, Guizhou 550025, PR China
[3] Key Laboratory of Efficient Utilization of Mineral and Green Chemical Technology, Guiyang, Guizhou 550025, PR China

[4] E-mail: jxcao@gzu.edu.cn

Abstract. The xonotlite crystals were synthesized via the hydrothermal synthesis manner from CaO and SiO_2 as the raw materials with their Si/Ca molar ratio of 1.0. Comparative dynamics analysis on xonotlite spherical particles synthesized via hydrothermal synthesis process was explored in this paper. The accuracy of the dynamic equation of xonotlite spherical particles was verified by two methods, one was comparing the production rate of the xonotlite products calculated by the dynamic equation with the experimental values, and the other was comparing the apparent activation energies calculated by the dynamic equation with that calculated by the Kondo model. The results indicated that the production rates of the xonotlite spherical particles calculated by the dynamic equation were in good agreement with the experimental values and the apparent activation energy of the xonotlite spherical particles calculated by dynamic equation (84 kJ·mol^{-1}) was close to that calculated by Kondo model (77 kJ·mol^{-1}), verifying the high accuracy of the dynamic equation.

1. Introduction

Xonotlite crystal belongs to monoclinic system (a=1.67nm, b=0.73nm, c=0.695nm), and it is a mineral of calcium silicate hydrate with the lowest crystalline water content, the best heat resistance and thermal stability (decomposition temperature of 1050-1100 ℃) [1-3]. In general, the xonotlite products used in industry were fabricated using dynamic process from CaO and SiO_2 as the raw materials with their Si/Ca molar ratio of 1.0 [4-19]. Due to the dissolution characteristics of siliceous material, the xonotlite crystals from H_2SiO_3 and K_2SiO_3 as siliceous materials could grow to form the various morphologies of spherical particles and fibers respectively [20]. In recent years, our group has completed the researches on the morphology and growth mechanism of xonotlite crystals [5, 7, 15 , 19, 20], moreover, by masterly measuring the pH and the calcium concentrations of product slurries, our group achieved the dynamic test of xonotlite spherical particles and pointed out that the dynamic equation of xonotlite spherical particles synthesized via hydrothermal synthesis process was of $-dc_A / dt = kc_A^{0.9}$, but the verification of this conclusion was not enough. Accordingly, in this paper, with H_2SiO_3 solution and $Ca(OH)_2$ suspension as siliceous material and calcareous material respectively, comparative dynamics analysis on xonotlite spherical particles synthesized via

hydrothermal synthesis process was explored by taking the Kondo model ($[1-(1-\alpha)^{1/3}]^A = k(t-t_0)$) into account in this paper, aiming to verify the accuracy of the dynamic equation of xonotlite spherical particles.

2. Experiment

2.1. Materials and methods

The xonotlite spherical particles were synthesized via the dynamic hydrothermal synthesis method. H_2SiO_3 solution and $Ca(OH)_2$ suspension were used as siliceous material and calcareous material respectively. $Ca(OH)_2$ suspension was prepared by mixing $CaCl_2$ with KOH 100g·L^{-1} at the molar ratio of 1:2. The calcareous material, distilled water, and siliceous material were homogeneously mixed, and then the mixture was transferred into a reaction chamber with a stirrer at a heating rate of 1.5 ℃·min^{-1} and a stirring rate of 200 rpm. The hydrothermal treatment proceeded under the following conditions: the Ca/Si molar ratio of 1.0, the reaction temperature of 190 ℃, 210 ℃ and 230 ℃ respectively. After the hydrothermal treatment, the suspensions were filtrated and washed three times by distilled water. The resultant powders were dried at 75 ℃ for 12 h. Technological flow diagram of hydrothermally synthesizing xonotlite products was shown in figure 1.

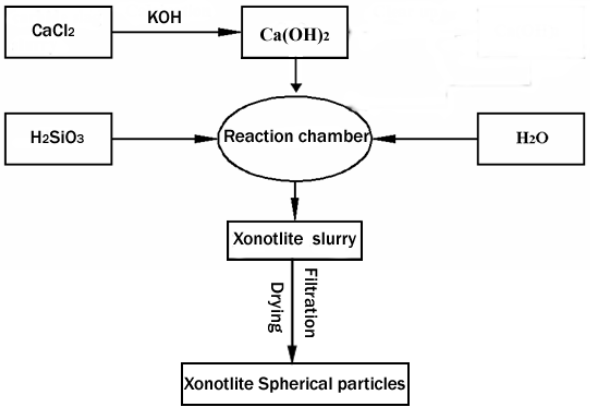

Figure 1. Technological flow diagram of hydrothermally synthesizing xonotlite spherical particles.

In this paper, the accuracy of the dynamic equation of xonotlite spherical particles synthesized via the dynamic hydrothermal synthesis method was verified by two methods, one was comparing the production rate of the xonotlite products calculated by the dynamic equation with the experimental values, and the other was comparing the apparent activation energies calculated by the dynamic equation with that calculated by the Kondo model ($[1-(1-\alpha)^{1/3}]^A = k(t-t_0)$).

2.2. The Determination Method of Samples

The reaction equation for the formation of the xonotlite spherical particles could be simplified as equation (1).

$$6Ca(OH)_2 + 6H_2SiO_3 + H_2O \rightarrow 6CaO \cdot 6SiO_2 \cdot H_2O + 12H_2O \quad (1)$$

Due to the invisibility of the hydrothermal synthesis reaction, it was impossible to observe the reaction process directly. With H_2SiO_3 solution and $Ca(OH)_2$ suspension as siliceous material and calcareous material respectively, the dynamic test of the hydrothermal synthesis process of the xonotlite spherical particles can be achieved by measuring the change of the pH during the reaction process.

The product slurries synthesized by hydrothermal synthesis process at various reaction temperatures and time were kept at 25 ℃ in thermostat water bath cauldron, and the pH of various slurries were measured using a PHS-3C precise pH meter. The product slurries were accurately

weighed by FA2004 electronic balance after drying. After the induction time (t_0), the qualities of the products obtained under various reaction times can be defined as m(Total)=m(HCl)+m($Ca(OH)_2$)+m(C-S-H(I))+m(xonotlite). A scanning electron microscope (SEM, Model JSM-6490LV, operating at 25 KV, Japan) was used to observe the morphologies of xonotlite crystals.

3. Results and discussion

Figure 2 shows the SEM images of the products hydrothermally synthesized from H_2SiO_3 as siliceous material via the dynamic processes at 190 ℃, 210 ℃ and 230 ℃ respectively.

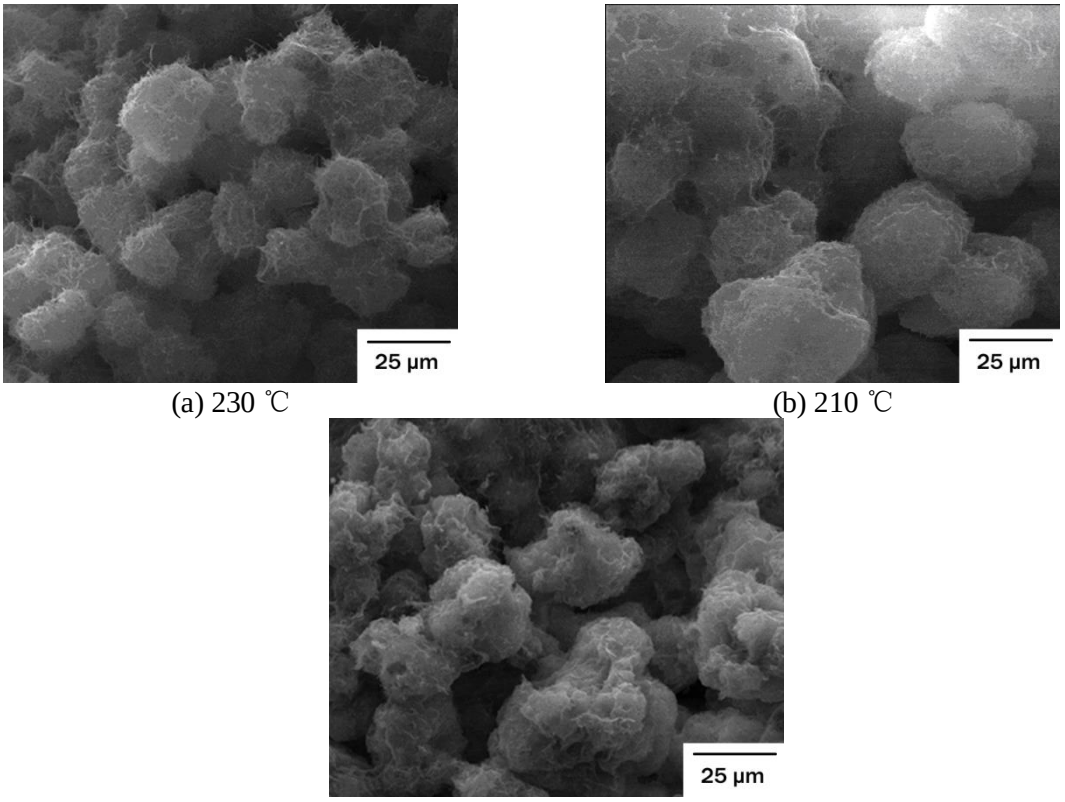

(a) 230 ℃ (b) 210 ℃

(c) 190 ℃

Figure 2. SEM images of the products hydrothermally synthesized from H_2SiO_3 as siliceous material at various temperatures.

In the hydrothermal synthesis process of xonotlite spherical particles, the reaction process can be expressed by the following reaction steps:

$$Ca(OH)_2 + H_2SiO_3 + H_2O \rightarrow C-S-H(gel) \quad (2)$$

$$C-S-H(gel) + Ca(OH)_2 + H_2SiO_3 + H_2O \rightarrow C-S-H(\text{II}) \quad (3)$$

$$C-S-H(\text{II}) + Ca(OH)_2 + H_2SiO_3 + H_2O \rightarrow C-S-H(\text{I})(5CaO\cdot 6SiO_2\cdot 5H_2O) \quad (4)$$

$$Ca(OH)_2 + C-S-H(\text{I})(5CaO\cdot 6SiO_2\cdot 5H_2O) \rightarrow 6CaO\cdot 6SiO_2\cdot H_2O + 5H_2O \quad (5)$$

The pH of the system were respectively measured after various reaction times, shown in figure 3. It can be seen from figure 3, with prolonging reaction time, the pH of hydrothermally synthesized products at various temperatures decreased, and its descending trend can be divided into three stages, that was, the stage forming amorphous C-S-H gels (equation (2, 3 and 4)), the stage forming the most of spherical xonotlite crystals (equation (5)), the stage forming a little xonotlite spherical particles.

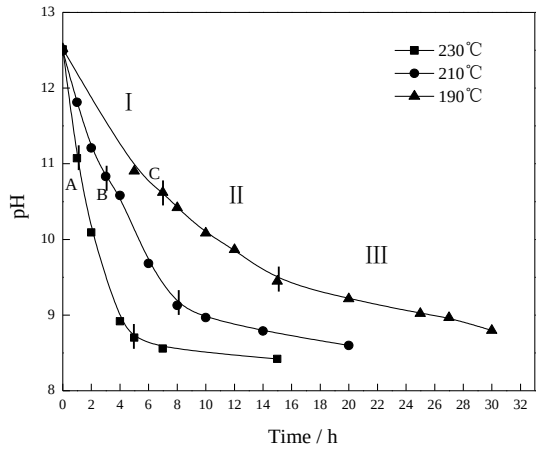

Figure 3. Time dependence of the pH of hydrothermally synthesized products at various temperatures.

Based on chemical reaction dynamic, using fourth-order Runge-Kutta method, spline interpolation and least-squares fitting method, the dynamic equation of xonotlite spherical particles synthesized via hydrothermal synthesis process was:

$$-dc_A / dt = kc_A^{0.9} \tag{6}$$

The dynamic equation (6) was a differential form which was easy to carry out the theoretical analysis. In practical applications, it was necessary to know the relationship between the production rate and the reaction time, thus this required the differential form to be transformed into integral form. The integral form of dynamic equation can be obtained by integrating the differential form of dynamic equation (6).

$$10C_{A,t0}^{0.1}[1-(1-\alpha)^{0.1}] = k(t-t_0) \tag{7}$$

In the equation： α —the production rate of the xonotlite spherical particles

t_0—the induction time

k—the rate constant

The values of t_0 and k are related to the reaction temperature.

The production rates of the xonotlite spherical particles calculated by the dynamic equation (7) were compared with the experimental values, shown in figure 4. Obviously, the calculated values were in good agreement with the experimental values, verifying the high accuracy of the dynamic equation (6).

According to the indefinite integral form of Arrhenius (Arrhenius S A) equation (8), if the values of the rate constants (k) at various temperatures was known, the diagram of $\ln k$—$1/T$ could be drawn and it should be a straight line, then the apparent activation energy (Ea) could be obtained from the slope and intercept of the straight line.

$$\ln k = -\frac{Ea}{RT} + \ln A \tag{8}$$

In the equation： k—the rate constant

A—the apparent frequency factor, the unit of it is the same as that of k

Ea—the apparent activation energy, the unit of it is J·mol^{-1}

R—the molar gas constant

T—the thermodynamic temperature

The fitted values of dynamic parameters (k) at various temperatures were shown in table 1.

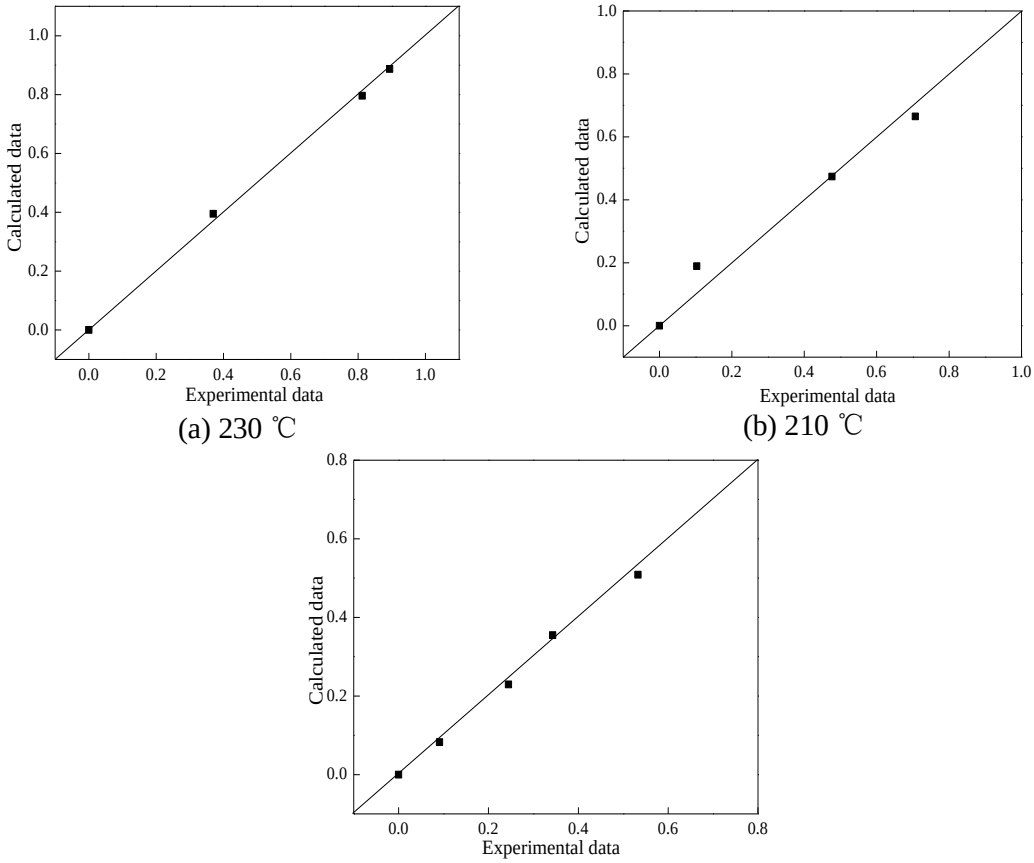

(a) 230 ℃ (b) 210 ℃

(c) 190 ℃

Figure 4. The experimental data comparison with calculated data of xonotlite spherical particles hydrothermally synthesized at various temperatures.

Table 1. The fitted values of *k* at various temperatures.

Temperature /℃	k / (mol m^{-3})$^{1/10}$ s^{-1}
230	0.3147
210	0.1330
190	0.0549

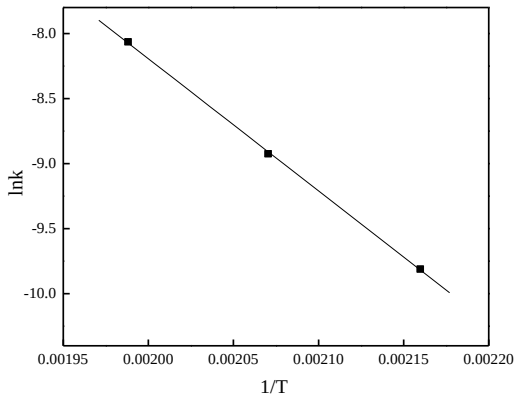

Figure 5. The $1/T$ dependence of $\ln k$ of hydrothermally synthesized xonotlite spherical particles.

According to the data shown in table 1 and equation (8), the diagram of $\ln k$—$1/T$ could be drawn, as shown in figure 5. Finally, the apparent activation energy (*Ea*) calculated by above-mentioned

method was of 84 kJ·mol^{-1}. Through above analysis we can infer that the change of the pH on the curve in the second stage might reflect the production rates of xonotlite crystals. Therefore, the starting points A, B and C of the second stage could be treated as the benchmark of the formation of xonotlite crystal at the hydrothermal synthesis temperature of 230 ℃, 210 ℃ and 190 ℃ respectively. With the process of reaction, the pH in the third stage tended to a fixed value, then the production rates of hydrothermal synthesis products (α) at various holding time can be obtained by setting this fixed value as the benchmark which indicated the complete formation of xonotlite crystals.

$$\alpha = \frac{pH_0 - pH}{pH_0 - pH_1} \tag{9}$$

In the equation： pH —the pH of product slurries synthesized via hydrothermal synthesis at various holding time

pH_0 —the pH of product slurries in the second stage when the xonotlite crystals began to form

pH_1 —the final constant pH of the product slurries synthesized via hydrothermal synthesis in the third stage

As shown in figure 6, the production rates of xonotlite crystals synthesized at various holding time could be calculated by equation (9).

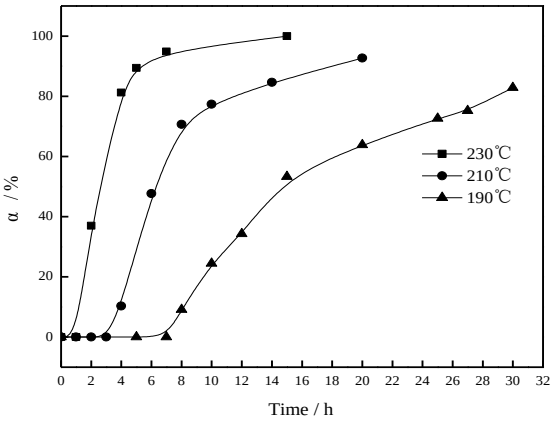

Figure 6. Time dependence of the conversion of hydrothermally synthesized products at various temperatures.

The second stage of the curve in figure 3 was analyzed and discussed by Kondo model commonly used for the hydrothermal reaction of lime-quartz system:

$$[1-(1-\alpha)^{1/3}]^A = k(t-t_0) \tag{10}$$

In the equation：A=1 or 2 respectively expressed that the interface reaction of crystal dominated the reaction rate and the diffusion controlled the reaction rate.

If the activation energy of the reaction was extremely small, the reaction rate was quite fast, then the reaction rate was dominated by the diffusion, on the contrary, if the activation energy of the reaction was extremely large, the reaction rate was quite slow, then the reaction rate was controlled by the interface reaction of crystal. In the studies of dynamic hydrothermal synthesis, Hongxun Liang and Hiroaki Noma have calculated that the xonotlite crystal has a large nucleation energy (117-118kJ·mol^{-1}), so the reaction rate was dominated by the interface reaction of crystal. Accordingly, the value of A was 1 in the equation (10) and the equation (10) could be simplified as:

$$[1-(1-\alpha)^{1/3}] = k(t-t_0) \tag{11}$$

As shown in figure 7, the relationship between the various holding time and 1-(1-α)$^{1/3}$could be obtained by applying the equation of Kondo model (11), then the corresponding regression rate parameter k, the induction time t_0 and its correlation coefficient γ could be obtained by regression analysis, shown in table 2. As can be seen from table 2, as the temperature decreased, the induction time increased. The induction time was the period required for the nucleation of the crystal at a certain

temperature, and its reciprocal could represent the growth rate of the crystal nucleus. Therefore, the decrease of temperature resulted in the decrease of the rate of crystal growth.

Thus, as shown in figure 8, the diagram of $\ln k$ —$1/T$ could be drawn by using the values of k at various temperature in table 2, then the apparent activation energy (Ea) could be calculated to be of 77 kJ·mol^{-1}.

Table 2. The regression rate parameter, induction time and correlation coefficient.

Temperature /℃	k / ×10^{-3}min^{-1}	t_0 / min	γ
230	2.23	57	0.99819
210	1.15	191	0.99589
190	0.46	416	0.99822

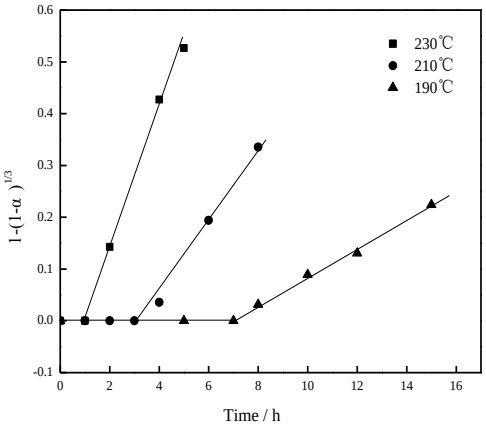

Figure 7. $1-(1-\alpha)^{1/3}$ versus time of Kondo model.

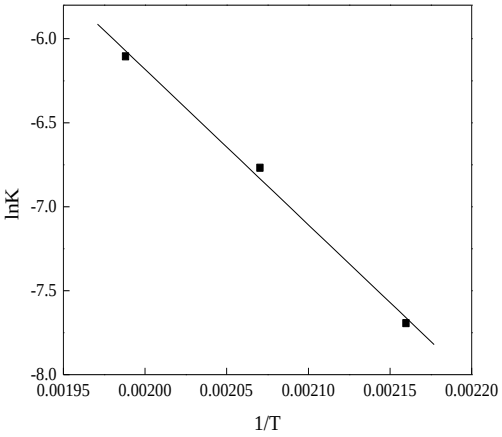

Figure 8. $\ln k$ versus $1/T$ of Kondo model.

Table 3. The apparent activation energy of hydrothermally synthesized xonotlite spherical particles.

Models	Apparent activation energy (Ea) / kJ mol^{-1}
$10C_{A,0}^{0.1}[1-(1-\alpha)^{0.1}]=k(t-t_0)$	84
$[1-(1-\alpha)^{1/3}]=k(t-t_0)$	77

The apparent activation energies of the xonotlite spherical particles calculated by dynamic equation (7) and equation of Kondo model (11) respectively were shown in table 3. The data of table 3 indicated that the apparent activation energy of the xonotlite spherical particles (84 kJ·mol^{-1}) calculated by dynamic equation was close to that (77 kJ·mol^{-1}) calculated by Kondo model. This result further verified the high accuracy of the dynamic equation (6).

4. Conclusions

(1) According to the three stages of the reaction process of xonotlite spherical particles, the change of the pH on the curve in the second stage could reflect the production rates of xonotlite crystals. The accuracy of the dynamic equation of xonotlite spherical particles was verified by comparing the activation energies calculated by the Kondo model.

(2) The production rates of the xonotlite spherical particles calculated by the dynamic equation were in good agreement with the experimental values, verifying the high accuracy of the dynamic equation.

(3) The apparent activation energy of the xonotlite spherical particles calculated by dynamic equation (84 kJ·mol^{-1}) was close to that calculated by Kondo model (77 kJ·mol^{-1}), further verifying the high accuracy of the dynamic equation.

Acknowledgments
We gratefully acknowledge the supports of this work by the National Natural Science Foundation of China (Grant No. 21666007), Science Technology Foundation of Guizhou (Grant No. 2014-2007) and Program for "Hundred" High-level Talents in Guizhou (Grant No. 2016-5655).

References
[1] Churakov S V and Mandalie P 2008 *Cement. Concrete. Res* **38** 300-11
[2] Dachowskia R and Stępień A 2011 *Procedia Engineering* **21** 1173-8
[3] Wei G S, Zhang X X and Yu F 2009 J. *Therm. Sci* **18** 142-9
[4] Zou J, Guo C, Jiang Y, Wei C and Li F 2016 *Mater. Chem. Phys* **172** 121-8
[5] Liu F, Zhu B and Cao J X 2011 *Adv. Mater. Res* **148-149** 1755-8
[6] Yang J, Zhang X, Ma H W, Wang M W and Wu H 2014 *Key Eng. Mater* **633** 7-10
[7] Liu F, Wang X D and Cao J X 2013 *Mater. Int. J. Miner. Metall. Mater* **20** 88-93
[8] Hartmann A, Schulenberg D and Buhl J C 2015 *J. Mater. Sci. Chem. Eng* **3** 39-55
[9] Spudulis E, Šavareika V and Špokauskas A 2013 *Mater. Sci-medzg* **19** 190-6
[10] Zou J J, Guo C B, Wei C D and Jiang Y S 2015 *Res Chem Intermed* **18** 1-12
[11] Guo X Y, Ma S H, Lü S Q, Zheng S L and Zou X 2015 *Chin. J. Nonferrous. Metals* **25** 534-44
[12] Yue H Z, Wang X, Yang Z Z and Wei C C 2017 *Key. Eng. Mater* **726** 569-75
[13] Black L, Garbev K and Stumm A 2009 *Adv. Appl. Ceram* **108** 137-44
[14] Liang H X and Li M Q 2002 *J. Chin. Ceram. Soc* **30** 294-9
[15] Liu F, Zeng L K, Cao J X and Li J 2010 *J. Wuhan. Univ. Technol* **25** 295-7
[16] Kurdowski W 2014 *Cement and Concrete Chemistry* (Dordrecht: Springer Netherlands) pp 205-77
[17] Shaw S, Clark S M and Henderson C M B 2000 *Chem. Geol* **167** 129-40
[18] Milestone N B and Ahari G K 2007 *Adv. Appl. Ceram* **106** 302-8
[19] Liu F, Chen S, Lin Q, Wang X D and Cao J X 2017 *Optoelectron. Lett* **13** 81-3
[20] Liu F, Wang X D and Cao J X 2011 *Adv. Mater. Res* **382** 379-83